International Journal of Pharmaceutics 389 (2010) 213–222

Contents lists available at ScienceDirect

International Journal of Pharmaceutics

journal homepage: www.elsevier.com/locate/ijpharm

Pharmaceutical Nanotechnology

Novel self-associating poly(ethylene oxide)-*b*-poly(ε-caprolactone) based drug conjugates and nano-containers for paclitaxel delivery

Mostafa Shahin[a], Afsaneh Lavasanifar[a,b,*]

[a] Faculty of Pharmacy and Pharmaceutical Sciences, University of Alberta, Edmonton, Alberta T6G 2N8, Canada
[b] Department of Chemical and Material Engineering, University of Alberta, Edmonton, Alberta T6G 2V4, Canada

ARTICLE INFO

Article history:
Received 25 September 2009
Received in revised form
24 December 2009
Accepted 10 January 2010
Available online 18 January 2010

Keywords:
Paclitaxel
Polymeric micelles
Polymer–drug conjugate
Poly(ethylene oxide)-*block*-poly(ε-caprolactone)

ABSTRACT

Poly(ethylene oxide)-*block*-poly(ε-caprolactone) (PEO-*b*-PCL) copolymers bearing paclitaxel (PTX) side groups on PCL (PEO-*b*-P(CL-PTX) were synthesized and assembled to particles of 123 nm average diameter. At 20% (w/w) PTX to polymer conjugation, PEO-*b*-P(CL-PTX) demonstrated only 5.0 and 6.7% PTX release after 72 h incubation at pH 7.4 and 5.0, respectively, but revealed signs of chain cleavage at pH 5.0. The cytotoxicity of PEO-*b*-P(CL-PTX) against MDA-MB-435 cancer cells increased as incubation time was raised from 72 to 96 h (IC_{50} of 680 and 475 ng/mL, respectively), but it was still significantly lower than the cytotoxicity of free PTX (IC_{50} of 3.5 ng/mL at 72 h). In further studies, micelles of PEO-*b*-PCL and those bearing benzyl or PTX on PCL were used for physical encapsulation of PTX, where maximum level of loading was achieved by PEO-*b*-P(CL-PTX) (2.22%, w/w). The release of PTX from this carrier was rapid; however. The *in vitro* cytotoxicity of physically loaded PTX was independent of carrier and similar to that of free PTX. This was attributed to the low concentration of polymers which fell below their critical micellar concentration in the cytotoxicity study. The results point to the potential of chemically tailored PEO-*b*-PCL for optimum PTX solubilization and delivery.

1. Introduction

Paclitaxel (PTX), is an antineoplastic drug successfully used against a variety of tumors including ovarian, breast and non-small cell lung tumors in clinic (Gregory and DeLisa, 1993; Wall and Wani, 1995; Chen et al., 2003). However, the main difficulty in its clinical use is its limited solubility in water (0.3 μg/mL) and many other acceptable pharmaceutical solvents (Sharma et al., 1995; Goldspiel, 1997). The commercial injectable formulation of PTX, Taxol®, utilizes a mixture of Cremophor EL and ethanol (1:1, v/v) (Singla et al., 2002). This formulation requires in-line filtration and should not be allowed to contact with plasticized polyvinyl chloride (PVC) devices as Cremophor EL is known to leach phthalate plasticizer (Mazzo et al., 1997; Boyle and Goldspiel, 1998). Also, the high amount of Cremophor EL in Taxol® results in hypersensitivity reactions, nephrotoxcicity, and neurotoxcicity (Onetto et al., 1993). It has been reported that Cremophor EL can modify the pharmacokinetics of PTX (Sparreboom et al., 1999). To overcome these problems, several alternative pharmaceutical carriers have been developed for PTX delivery (Singla et al., 2002; Edelman, 2009).

We report on the development of new self-associating block copolymer–PTX conjugates and nano-containers based on functionalized poly(ethylene oxide)-*block*-poly(ε-caprolactone) (PEO-*b*-PCL) for the solubilization and delivery of PTX. Conjugation of small molecule drugs to macromolecular carriers to produce polymer–drug conjugates has proven to be a valuable formulation strategy for anticancer agents (Duncan, 2006). To date, two PTX polymeric conjugates, i.e., PNU166945 and Xyotax™ (CT-2103) have entered clinical trials (Duncan, 2003). In PNU166945, PTX is linked to hydroxypropyl methacrylamide polymer through formation of an ester bond with a short peptide linker (Gly-Phe-Leu-Gly). PNU166945 has shown poor pharmacokinetics in phase I clinical trials due to instability of ester linkage conjugating PTX (Meerum Terwogt et al., 2001). Xyotax™, polyglutamic acid (PGA) conjugated to PTX through an ester linkage, is the only PTX polymeric conjugate in phase III clinical trials for the treatment of non-small cell lung cancer in combination with carboplatin (Singer et al., 2003; Langer, 2004; Singer, 2005). In general polymer–drug conjugates offer potential advantages over Taxol®, first they eliminate the need for toxic solubilizing agent (Cremophor EL) and enhance the tumor tissue uptake through Enhanced Permeation and Retention (EPR) effect, as well as they show better pharmacokinetic profile and less toxicity due to limited normal tissue exposure to free drug (Singer et al., 2005).

In this study, the block copolymer–PTX conjugate was synthesized through formation of an ester bond between a hydroxyl

* Corresponding author at: Faculty of Pharmacy and Pharmaceutical Sciences, University of Alberta, Edmonton, Alberta T6G 2N8, Canada. Tel.: +1 780 492 2742; fax: +1 780 492 1217.
E-mail address: alavasanifar@pharmacy.ualberta.ca (A. Lavasanifar).

0378-5173/$ – see front matter © 2010 Elsevier B.V. All rights reserved.
doi:10.1016/j.ijpharm.2010.01.015

group in PTX and free side carboxyl groups on poly(ethylene oxide)-*block*-poly(α-carboxyl-ε-caprolactone) (PEO-*b*-PCCL) producing PEO-*b*-P(CL-PTX). This block copolymer–PTX conjugate contains several side PTX molecules on the hydrophobic block of one polymer chain and readily assembles to polymeric nanoparticles. The ester bond between PTX and polymeric backbone was expected to be protected within the hydrophobic core of nano-carriers preventing premature drug release within the systemic circulation. A similar approach has been used to form block copolymer conjugates of doxorubicin (DOX) through formation of amide bonds between free amino group of DOX and PEO-*b*-PCCL in our previous publication (Mahmud et al., 2008). As an alternative to chemical conjugation of PTX to self-associating block copolymers, PEO-*b*-PCL, PEO-*b*-poly(α-benzyl carboxylate-ε-caprolactone) (PEO-*b*-PBCL) and PEO-*b*-P(CL-PTX) were self-assembled to polymeric nano-carriers and used for physical encapsulation of PTX, as well.

2. Materials and methods

2.1. Materials

Methoxy polyethylene oxide (average molecular weight of 5000 g mol^{-1}), diisopropyl amine (99%), benzyl chloroformate (tech. 95%), sodium (in Kerosin), Butyl Lithium (Bu-Li) in hexane (2.5 M solution), palladium coated charcoal, N,N dicylcohexyl carbodiimide (DCC), dimethylamino pyridine (DMAP), and pyrene were purchased from Sigma chemicals (St. Louis, MO, USA). Paclitaxel (purity > 99.5) was purchased from LC Laboratories (Woburn, MA, USA). ε-caprolactone was purchased from Lancaster Synthesis, UK. Stannous octoate was purchased from MP Biomedicals Inc., Germany. Fluorescent probes, pyrene and 1,3-(1,1′-dipyrenyl)propane were purchased from Molecular Probes, USA. Cell culture media RPMI 1640, penicillin–streptomycin, fetal bovine serum, and L-glutamine were purchased from GIBCO, Invitrogen Corp. (Burlington, ON, Canada). All other chemicals were reagent grade.

2.2. Methods

2.2.1. Synthesis of PEO-b-PCL and PEO-b-PBCL block copolymers

PEO-*b*-PCL block copolymer was synthesized by ring opening polymerization of ε-caprolactone using methoxy polyethylene oxide as initiator and stannous octoate as catalyst. Methoxy PEO (M_W: 5000 g mol^{-1}) (0.5 g), ε-caprolactone (0.5 g) and stannous octoate (0.002 eq of monomer) were added to dry 10 mL ampoule nitrogen purged and sealed under vacuum. The reaction was carried out by placing the ampoule at 140 °C for 4 h in oven and terminated by cooling the product to room temperature (Mahmud et al., 2006). For the synthesis of PEO-*b*-PBCL, methoxy PEO (M_W: 5000 g mol^{-1}) (3.5 g), α-benzylcarboxylate-ε-caprolactone (3.5 g) and stannous octoate (0.002 eq of monomer) were used as initiator, monomer and catalyst under identical reaction condition. The synthesis of functionalized monomer, i.e., α-benzyl carboxylate-ε-caprolactone is reported in a previous paper (Mahmud et al., 2006). Briefly, to a solution of 60.0 mmol of dry diisopropylamine in of dry THF, 60.0 mmol of Butyl Lithium in hexane were slowly added at −30 °C under vigorous stirring with continuous argon supply. The solution was cooled to −78 °C and kept stirring for additional 20 min. Freshly distilled ε-caprolactone (30 mmol) was dissolved in dry THF and added to the above mentioned mixture slowly, followed by the addition of benzyl chloroformate (30 mmol). The temperature was allowed to rise to 0 °C after 1.5 h and the reaction was quenched with 5 mL of saturated ammonium chloride solution. The reaction mixture was diluted with water and extracted with ethyl acetate. The combined extracts were dried over Na_2SO_4 and purified by column chromatography using an eluant of 25% ethyl acetate in hexane.

2.2.2. Synthesis of PEO-b-P(CL-PTX)

The synthesis of PEO-*b*-P(CL-PTX) was accomplished in two steps (Scheme 1). In the first step, PEO-*b*-PCCL was synthesized through catalytic debenzylation of PEO-*b*-PBCL in the presence of hydrogen gas as reducing agent and palladium coated charcoal as catalyst according to a procedure described before (Mahmud et al., 2006). In the second step, PTX was chemically conjugated to PEO-*b*-PCCL through formation of an ester bond by a DCC and DMAP mediated coupling reaction (Li and Kwon, 1999). Briefly, DMAP (17.7 mg, 0.145 mM) and DCC (29.9 mg, 0.145 mM) were added to a stirred solution of PEO-*b*-PCCL (M_W: 6900 g mol^{-1}) (100 mg, 0.0145 mM) in anhydrous dichloromethane (DCM) (20 mL). Subsequently, after stirring for 30 min PTX (37.1 mg, 0.0435 mM) in 1 mL of dried DCM was added. The reaction was carried out under argon gas while protected from light for 4 days at room temperature. Thin layer chromatography (TLC) in the presence of THF: DCM (1:4) as the mobile phase was used to monitor the reaction progress and spots were detected by a UV lamp at 254 nm (Vaisman et al., 2005). The by-product dicyclohexyl urea was filtered out. The product was condensed by bubbling of nitrogen gas. The purification of the polymer from free PTX was carried out by dialysis against 1 L of dimethlyl sulphoxide (DMSO) for one day, then against double distilled water for another day using cellulose membrane (Spectrapore, cutoff M_W: 3500 g mol^{-1}). The PTX conjugated block copolymer, i.e., PEO-*b*-P(CL-PTX), was then lyophilized to a white powder. The prepared copolymer was characterized for its average molecular weights and polydispersity by ^{1}H NMR and Gel permeation chromatography (GPC). ^{1}H NMR was carried out by Bruker Unity-300 spectrometer at room temperature, using deuterated chloroform ($CDCl_3$) as solvent and tetramethyl silane as internal reference standard. The GPC was carried out at 25 °C with an HP instrument equipped with Waters Styragel HT4 column (Waters Inc., Milford, MA). The elution pattern was detected at 35 °C by refractive index (PD 2000, precision detector, Inc.)/light scattering (model 410, Waters Inc.) detectors. THF (1 mL/min) was used as eluent. Samples of 20 μL from 10 mg/mL polymer solution in THF were injected. The column was calibrated with a series of standard polystyrenes. The PTX content in the conjugate was calculated from the ^{1}H NMR spectrum using the peak intensity of phenyl protons signal at (7.3–8.4 ppm) and the ethylene proton signal (3.7 ppm).

2.2.3. Self-assembly of block copolymers and physical encapsulation of PTX in the assembled structures

Self-assembly of PEO-*b*-P(CL-PTX) was accomplished through dialysis method. The block copolymer (3 mg) was dissolved in DMSO (0.5 mL). This solution was added to doubly distilled water (3 mL) in a drop-wise manner under moderate stirring for 1 day followed by organic solvent removal by dialysis against double distilled water for another day (Spectrapor, M_W cutoff 3500 g mol^{-1}). This solution was then centrifuged 11,600 × *g* for 5 min to remove any free unimers.

Encapsulation of PTX in PEO-*b*-PCL, PEO-*b*-PBCL and PEO-*b*-P(CL-PTX) micelles was carried out by an identical procedure with the exception that the polymer and PTX were dissolved in N-N, dimethyl formamide (DMF) as an organic solvent and the final polymer concentration was adjusted to 0.36 mM (Letchford et al., 2009). To determine the maximum loading of PTX in micelles, several micellar formulations were prepared with increasing amounts of PTX in DMF/copolymer solution. After dialysis, the solution was centrifuged at 11,600 × *g* for 5 min to remove any precipitate, and an aliquot (100 μL) of the micellar solution was diluted with acetonitrile. The solution was analysed for PTX content using

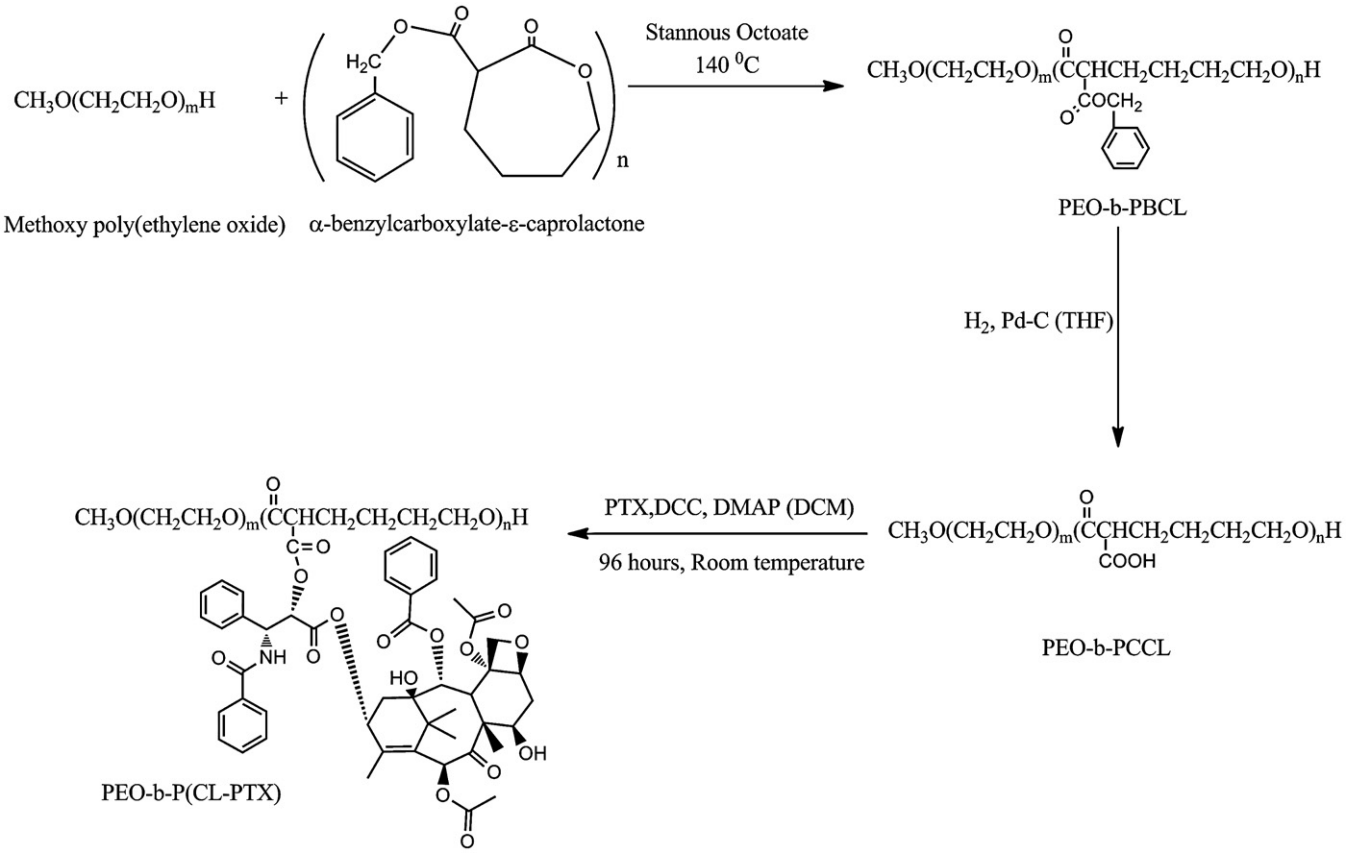

Scheme 1. Synthesis of PEO-*b*-P(CL-PTX) block copolymer.

HPLC. Varian prostar 210 HPLC system at a flow rate of 1.0 mL/min at room temperature was used. The detection was performed at 227 nm using a Varian 335 Photodiode Array HPLC detector (Varian Inc., Australia). Reversed phase chromatography was carried out with a Microsorb-MV 5 μm C18-100 Å column (4.6 mm × 250 mm) with 20 μL of sample injected in a gradient elution using 0.1% trifluroacetic acid aqueous solution and acetonitrile. The percent of acetonitrile was 40% at time and increased with elution time up to 100% within 15 min (Forrest et al., 2008). The level of PTX loading (w/w%), (mol/mol%) and encapsulation efficiency were calculated using the following Eqs. ((1)–(3)):

$$\text{PTX loading (w/w\%)} = \frac{\text{amount of physically loaded PTX in mg}}{\text{amount of copolymer in mg}} \times 100 \quad (1)$$

$$\text{PTX loading (mol/mol\%)} = \frac{\text{amount of physically loaded PTX in moles}}{\text{amount of copolymer in moles}} \times 100 \quad (2)$$

$$\text{Encapsulation efficiency (\%)} = \frac{\text{amount of physically loaded PTX in mg}}{\text{amount of PTX added in mg}} \times 100 \quad (3)$$

2.2.4. Characterization of polymeric micelles

2.2.4.1. Critical micellar concentration. A change in the fluorescence excitation spectra of pyrene in the presence of varied concentration of PEO-*b*-P(CL-PTX) block copolymer was used to measure its CMC according to the method described previously (Zhao et al., 1990). Briefly, pyrene was dissolved in acetone and added to 5 mL volumetric flasks to provide a concentration of 6×10^{-7} M in the final solutions. Acetone was then evaporated and replaced with aqueous polymeric micellar solutions with concentrations ranging from 0.061 to 1000 μg/mL. Samples were heated at 65 °C for an hour, cooled to room temperature overnight, and deoxygenated with nitrogen gas prior to fluorescence measurements. The excitation spectrum of pyrene for each sample was obtained at room temperature using a Varian Cary Eclipse fluorescence spectrophotometer (Victoria, Australia). The scans was performed at medium speed (600 nm/min) and at a PMT detector voltage of 575 V. Emission wavelength and excitation/emission slit were set at 390 nm and 5 nm, respectively. The intensity ratio of peak at 338 nm to that at 333 nm was plotted against the logarithm of copolymer concentration. CMC was measured from a sharp rise in intensity ratios (I_{338}/I_{333}) at the onset of micellization.

2.2.4.2. Core viscosity. The viscosity of hydrophobic domain in the self-assembled structures was estimated by measuring excimer to monomer intensity ratio (I_e/I_m) from the emission spectra of 1,3-(1,1′-dipyrenyl)propane at 480 and 373 nm, respectively, in the presence of polymer solutions at 1 mg/mL concentration. The details of the method are described in a previous publication (Lavasanifar et al., 2001).

2.2.4.3. Micellar shape and size. The average diameter and size distribution of the prepared nano-carriers were estimated by dynamic light scattering (DLS) using Malvern Zetasizer 3000 after centrifugation at 11,600 × *g* for 5 min.

The morphology of PEO-*b*-P(CL-PTX) nano-carriers was determined by both transmission electron microscopy (TEM) and atomic force microscopy (AFM). The TEM experiment was carried out by

placing an aqueous droplet (20 μL) of the micellar solution with a polymer concentration of 1 mg/mL on a copper coated grid. The grid was held horizontally for 20 s to allow the colloidal aggregate to settle. Then, a drop of 2% solution of phosphotungstic acid in PBS was added to provide the negative stain. After 1 min, the excess fluid was removed by filter paper. The sample was then air dried and loaded into transmission electron microscope (Hitachi H 7000, Tokyo, Japan) (Lavasanifar et al., 2001).

The AFM experiment was carried out by placing an aliquot (2 μL) of the micellar solution (0.1 mg/mL) on a freshly cleaved mica surface (flogopite, $KMg_3AlSi_3O_{10}(OH)_2$) and air dried at room temperature. Samples were imaged in air at room temperature and humidity with MFP-3D inverted optical AFM (Digital Instruments, Santa Barbara, CA), equipped with a 120 μm *xy* and 6 μm *z* scanner for accurate length, height and force measurements. An integral silicon tip cantilever (OMCL-AC160TS-W2, Olympus Cantilevers) with a spring constant of 10 pN/nm was used. AFM tapping mode imaging was done at scan rates of 1–1.5 Hz/line and set point of 600 mV. All images were processed with a second-order flattening routine for background correction.

2.2.5. Evaluation of the physical stability of prepared nano-carriers

The PEO-*b*-P(CL-PTX) micellar solution (1 mg/mL) was prepared as described previously in phosphate buffer (0.01 M, pH 7.4) and left for 7 days at room temperature. At different time points, the hydrodynamic diameter as well as the polydispersity of the micellar solution was assessed using Malvern Zetasizer 3000 as described above. For physically encapsulated PTX nano-carriers, solutions in double distilled water were prepared at 0.36 mM polymer concentration. The possibility for the formation of secondary aggregates was then investigated by measuring the size of nano-carriers right after preparation.

2.2.6. Assessing the hydrolysis of poly(ester) backbone in PEO-b-P(CL-PTX)

PEO-*b*-P(CL-PTX) micellar solutions (1 mg/mL) in 0.01 M phosphate buffer (pH 7.4) and 0.01 M citrate buffer (pH 5.0) were prepared, and incubated in a closed vial at 37 °C in a Julabo SW 22 shaking water bath (Germany). After 72 h, the micellar solution was freeze dried and dissolved in THF. Aliquot of 20 μL from this solution was injected into the GPC system as described above.

2.2.7. Release of PTX from polymeric micelles

Release of PTX from the PEO-*b*-P(CL-PTX) conjugate was determined in 0.01 M phosphate buffer (pH 7.4) and 0.01 M citrate buffer (pH 5.0) containing 2 M sodium salicylate at 37 °C (Cho et al., 2004; Hu et al., 2006). The experiment was initiated by the addition of free or micellar PTX solution to the buffer to give a final PTX concentration of 25 μg/mL. At fixed time intervals, a sample of 1 mL was withdrawn, freeze dried and dissolved in acetonitrile, then 20 μL aliquot was injected into HPLC to determine the amount of released PTX.

The PTX loaded micelles were prepared at 20 μg/mL PTX concentration from PEO-*b*-PCL, PEO-*b*-PBCL and PEO-*b*-P(CL-PTX) block copolymers according to the previously mentioned method. Then, 10 mL of the micellar solutions were transferred into a dialysis bag (Spectrapor, M_W cutoff 3500 g mol^{-1}). The dialysis bags were placed into 500 mL of 0.01 M phosphate buffer (pH 7.4) or 0.01 M citrate buffer (pH 5.0). The release study was performed at 37 °C in a Julabo SW 22 shaking water bath (Germany). At selected time intervals the whole release media has been replaced with fresh one and aliquots of 200 μL were withdrawn from the inside of the dialysis bag for HPLC analysis. The amount of PTX released was calculated by subtracting the amount of PTX remained in the dialysis bag from the initially added PTX. The release profiles were compared using similarity factor, f_2, and the profiles were considered significantly different if $f_2 < 50$ (Costa and Sousa Lobo, 2001).

$$f_2 = 50 \times \log\left(\left[1 + \left(\frac{1}{n}\right)\sum_{j=1}^{n}|R_j - T_j|^2\right]^{-0.5} \times 100\right) \quad (4)$$

where n is the sampling number, R_j and T_j are the percent released of the reference and test formulations at each time point j.

2.2.8. In vitro cytotoxicity of physically encapsulated and chemically conjugated PTX against MDA-MB-435 cancer cells

The cytotoxicity of PEO-*b*-P(CL-PTX), PEO-*b*-PCCL and PTX loaded in PEO-*b*-PCL, PEO-*b*-PBCL and PEO-*b*-P(CL-PTX) block copolymer micelles against human MDA-MB-435 cancer cells was investigated using 3-(4,5-dimethylthiazol-2-yl)-2,5-diphenyltetrazolium bromide MTT assay. Cells were grown in RPMI 1640 complete growth media supplemented with 10% fetal bovine serum, 1% (w/v%) L-glutamine, 100 units/mL penicillin and 100 μg/mL streptomycin and maintained at 37 °C with 5% CO_2 in a tissue culture incubator. Growth medium RPMI containing 4000 cells was placed in each well in 96-well plate and incubated overnight to allow cell attachment. After 48 h (50% confluency), micellar solutions and free PTX at different concentrations were incubated with the cells for 24, 48 and 72 h. For conjugated PTX, a 96 h incubation period was also tried. After this time, MTT solution (20 μL; 5 mg/mL in sterile-filtered PBS) was added to each well and the plates were re-incubated for another 4 h. The formazan crystals were dissolved in DMSO, and the cell viability was determined by measuring the optical absorbance differences between 570 and 650 nm using a Power Wave X 340 microplate reader (Bio-Tek Instruments, Inc., USA). The mean and the standard deviation of cell viability for each treatment was determined, converted to the percentage of viable cells relative to the control. The concentration required for 50% growth inhibition (IC_{50}) was estimated from the plot of the percentage of viable cells versus log PTX concentration using Graphpad prism for Windows, Version 5.0 (Graphpad Software Inc.).

2.2.9. Statistical analysis

Values are presented as mean ± standard deviation (SD) of triple measurements. Statistical significance of difference was tested either using Students't test or one-way ANOVA test (Sigma plot for windows, Version 11.0, Systat software Inc.). The level of significance was set at $\alpha = 0.05$.

3. Results

3.1. Preparation and characterization of PEO-b-P(CL-PTX) nano-conjugates

Synthetic scheme for the preparation of PEO-*b*-P(CL-PTX) through conjugation of PTX to PEO-*b*-PCCL in the presence of DCC and DMAP is illustrated in Scheme 1. The 2′ and 7 hydroxyl groups of PTX are suitable sites for conjugation (Skwarczynski et al., 2006). The reaction is more likely to occur at the 2′ hydroxyl group since steric hindrances reduce the reactivity of the 7-hydroxyl group (Greenwald et al., 1994). The successful conjugation of PTX to PEO-*b*-PCCL was confirmed by TLC, where no spot for free PTX has been visualized in the TLC for the polymeric conjugate solution. Further evidence for conjugation was provided by comparing the ^{1}H NMR spectra of PEO-*b*-PCCL (Fig. 1A) to that of PTX and PEO-*b*-P(CL-PTX) (Fig. 1B and C, respectively), where characteristic peaks of PEO-*b*-PCCL and PTX were observed in the ^{1}H NMR spectrum of PEO-*b*-P(CL-PTX). Importantly, in the spectrum of PEO-*b*-P(CL-PTX)

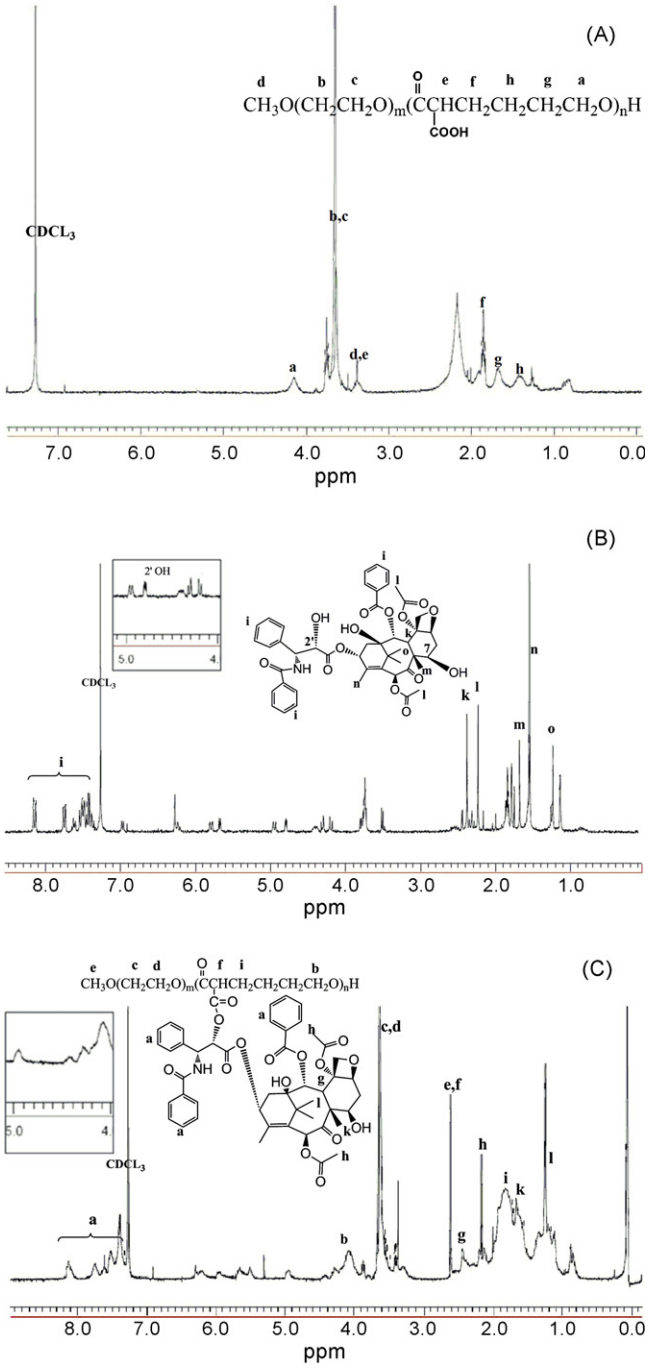

Fig. 1. ^{1}H NMR spectra of (A) PEO-*b*-PCCL, (B) PTX and (C) PEO-*b*-P(CL-PTX) in $CDCl_3$.

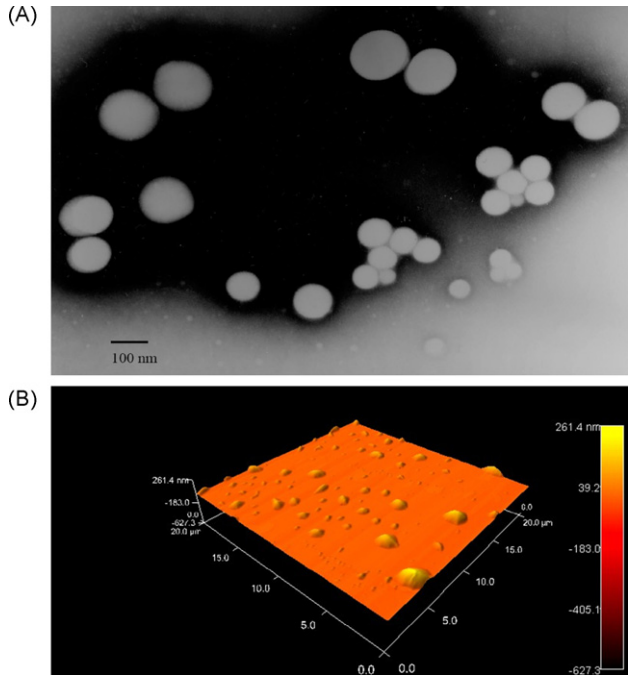

Fig. 2. (A) TEM and (B) AFM images of empty PEO-*b*-P(CL-PTX) nanoparticles.

the disappearance of the resonance at $\delta = 4.8$ ppm (s, 1H) which is observed in the spectrum of PTX and corresponds to the proton of the 2′-OH confirmed the completion of the conjugation reaction at this position (enlarged windows Fig. 1B and C). Furthermore, the GPC chromatogram of the PEO-*b*-P(CL-PTX) exhibited a single peak, which is left shifted compared to that of PEO-*b*-PCCL indicating the increase of molecular weight due to PTX conjugation. Also, the HPLC chromatogram of PEO-*b*-P(CL-PTX) block copolymer did not show free PTX peak (data not shown). Together, the results of TLC, ^{1}H NMR, HPLC along with GPC provided strong evidence for the conjugation of PTX to the PEO-*b*-PCCL and efficient removal of free PTX after the purification process. The PTX content in the conjugate calculated from comparing the peak intensity of the phenyl protons signal ($\delta = 7.3$–8.4 ppm) and ethylene protons ($\delta = 3.7$) of the poly(ethylene oxide) in the ^{1}H NMR (Fig. 1C) was ~20% by weight. The substitution level of PTX on the polymer on molar basis was ~22% (moles PTX/moles monomer). This corresponds to 1.79 PTX molecules per PEO_{114}-*b*-$P(CL\text{-}PTX)_8$ chain on average.

The results of characterization studies on prepared polymeric micelles are summarized in Table 1. The average hydrodynamic diameter of the unloaded PEO-*b*-P(CL-PTX) particles and their polydispersity were 123 ± 0.60 nm and 0.14 as determined by DLS technique, respectively. This was larger than the size of PEO-*b*-PCL, PEO-*b*-PBCL, PEO-*b*-PCCL micelles formed through a similar assembly process. To visualize the shape of the formed particles TEM and AFM images were obtained (Fig. 2A and B, respectively). From the TEM, spherical particles were observed with an average diameter of (105.0 ± 28.3 nm). AFM provided another evidence for the spherical morphology of particles with an average diameter of 87 nm. The CMC of PEO-*b*-P(CL-PTX) conjugate in aqueous media as estimated by pyrene partition study was 60.6×10^{-2} μM (Table 1). The PTX conjugated polymer showed significantly higher CMC in comparison to PEO-*b*-PCL ($P < 0.05$, unpaired Student's *t*-test) (Table 1). The higher CMC of PEO-*b*-P(CL-PTX) in comparison to that of PEO-*b*-PCL under this study, is attributed to the presence of free carboxyl groups and shorter chain length of the core forming block both leading to a decreased hydrophobicity of P(CL-PTX) in comparison to PCL. The lower CMC of PEO-*b*-P(CL-PTX) compared to that of PEO-*b*-PCCL is due to PTX conjugation on PCCL that makes the core forming block more hydrophobic.

Studying the core viscosity of both PEO-*b*-P(CL-PTX) and PEO-*b*-PCL using the fluorescence emission spectrum of 1,3-(1,1′-dipyrenyl)propane at a polymer concentration above CMC (1 mg/mL) revealed a lower core viscosity for PEO-*b*-P(CL-PTX) (Table 1). This is evidenced by the significantly higher I_e/I_m ratio for PEO-*b*-P(CL-PTX) (0.173) in comparison to PEO-*b*-PCL micelles (0.055) ($P < 0.001$, unpaired Student's *t*-test).

PEO-*b*-P(CL-PTX) micelles retained their average size and polydispersity over the 7 days incubation period ($P > 0.05$) indicating good stability of the plain PEO-*b*-P(CL-PTX) particles at room temperature (Fig. 3).

Table 1
Characteristics of prepared block copolymers and empty polymeric micelles ($n = 3$).

Block copolymer[a]	M_n (g mol^{-1})[b]	Polydispersity (M_w/M_n)[c]	Average micellar size[d] ± SD (nm)	PDI[e]	CMC [f] ± SD (uM)	I_e/I_m ± SD[g]
PEO_{114}-*b*-PCL_{42}	9790	1.097	62.5 ± 1.80	0.24	0.18 ± 0.010[h]	*0.055 ± 0.00*[h]
PEO_{114}-*b*-$PBCL_{18}$	9470	1.175	64.3 ± 3.50	0.34	N/D	*N/D*
PEO_{114}-*b*-$PCCL_{12}$	6900	1.321	89.5 ± 3.60	0.44	N/D	*N/D*
PEO_{114}-*b*-P(CL-PTX)$_8$	7770	1.285	123 ± 0.60	0.14	0.61 ± 0.014[*]	*0.173 ± 0.004*[*]

N/D: Not determined.
[a] The number showed as subscript indicates the polymerization degree of each block determined from ^{1}H NMR spectroscopy.
[b] Number average molecular weight measured by ^{1}H NMR.
[c] Polydispersity = M_w/M_n measured by GPC.
[d] hydrodynamic diameter estimated by dynamic light scattering.
[e] Polydispersity index estimated by dynamic light scattering.
[f] Critical micelle concentration measured from the rise in the intensity ratio of peaks at 338 nm to the peaks at 333 nm in the fluorescence excitation spectra of pyrene plotted versus logarithm of polymer concentration.
[g] Intensity ratio (excimer/monomer) from emission spectrum of 1,3-(1,1′-dipyrenyl)propane in the presence of polymeric micelle.
[h] The data are reproduced from reference Mahmud et al. (2008) for comparison.
[*] Statistically different from PEO-*b*-PCL ($P < 0.001$).

As shown in Fig. 4A, the release of intact PTX from the polymeric conjugate was very slow within 3 days at both pHs. After 72 h incubation, only 6.7% of total PTX were detected in media as intact PTX at pH 5.0 compared to 5.0% at PH 7.4. The lower level of free PTX at pH 7.4 may be attributed to the lower stability of PTX at this pH rather than a slower drug release from the conjugate. Similar reduction in the level of solubilized PTX has been seen at this pH for free drug. It has been reported that free PTX is susceptible to mild basic hydrolysis (Ringel and Horwitz, 1987).

Fig. 4B shows the GPC chromatogram of chemically conjugated PTX after incubation at pH 7.4 and 5.0 for 72 h. No significant change in the elution time of polymer–PTX conjugate after incubation at both pHs was seen indicating no change in its number average molecular weight. However, a change in its polydispersity upon incubation at pH 5.0 was observed implicating a decrease in the weight average molecular weight of the polymer–drug conjugate at this pH.

The cytotoxicity of free PTX, PEO-*b*-P(CL-PTX), PEO-*b*-PCCL against human MDA-MB-435 cancer cells using MTT assay is shown in Fig. 5. A change in cell viability with a change in the concentration of both free PTX and the PTX polymeric conjugate was observed. The conjugate showed lower cytotoxicity than free PTX (IC_{50} of 680 ng/mL for conjugate versus 3.5 ng/mL for free PTX) after 72 h incubation. The polymer without conjugated PTX, i.e., PEO-*b*-PCCL, did not show noticeable cytotoxicity at concentrations equivalent to what used in this study. When the incubation time increased to 96 h, the cytotoxicity of PTX polymeric conjugate increased (i.e. the IC_{50} decreased significantly from 680 to 475 ng/mL) ($P < 0.05$, unpaired Student's *t*-test).

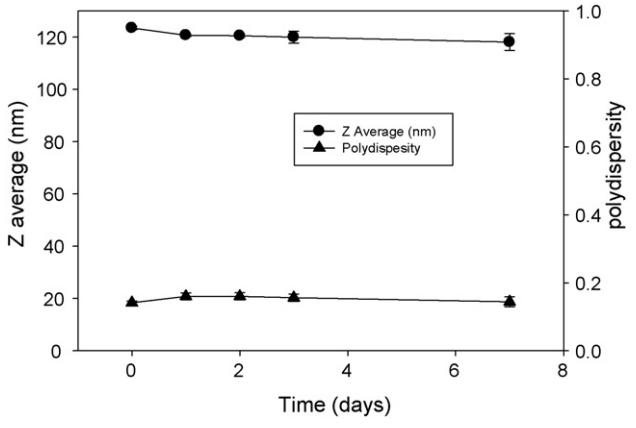

Fig. 3. The average diameter and polydispersity of PEO-*b*-P(CL-PTX) nanoparticcles during storage at room temperature as measured by dynamic light scattering (DLS).

3.2. Preparation and characterization of polymeric micelles containing physically encapsulated PTX

The capability of PEO-*b*-PCL, PEO-*b*-PBCL, and PEO-*b*-P(CL-PTX) micelles for the solubilization of PTX in aqueous media was investigated at different drug to polymer weight ratios (Fig. 6). Except for PEO-*b*-P(CL-PTX), all the prepared solutions were clear, up to a certain ratio, after which precipitation was evident by visual inspection. The amount of the drug solubilized increased to a maximum concentration for PEO-*b*-PCL and PEO-*b*-PBCL as the drug to polymer ratio was raised from 2 to 5 and 2 to 2.5 wt%, respec-

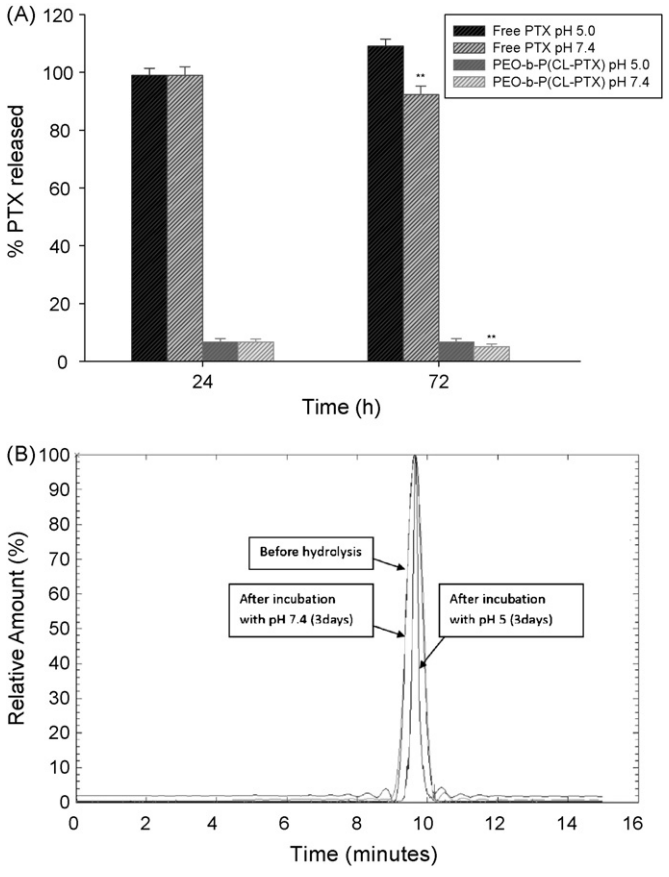

Fig. 4. (A) Percentage of intact PTX regenerated from PEO-*b*-P(CL-PTX) in buffer solutions (pH 7.4 and pH 5) containing 2 M sodium salicylate at 37 °C in comparison to free PTX. (B) Gel permeation chromatogram of PEO-*b*-P(CL-PTX) before and after incubation at pHs 7.4 and 5 for 72 h. Significantly different from pH 5 ($^{**}P < 0.05$).

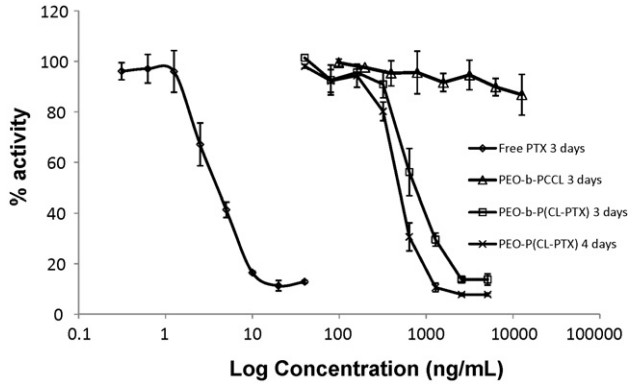

Fig. 5. *In vitro* cytotoxicity of PEO-*b*-P(CL-PTX), PEO-*b*-PCCL block copolymers and free PTX against MDA-435 cells at defined incubation times.

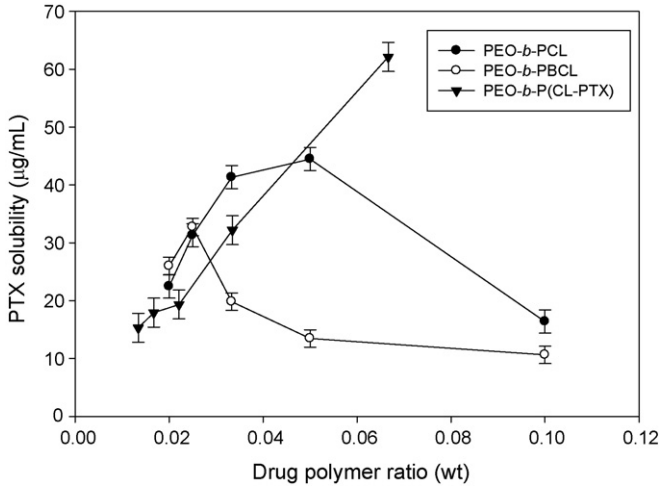

Fig. 6. Solubilization of PTX by block copolymers at different PTX:block copolymers weight ratios.

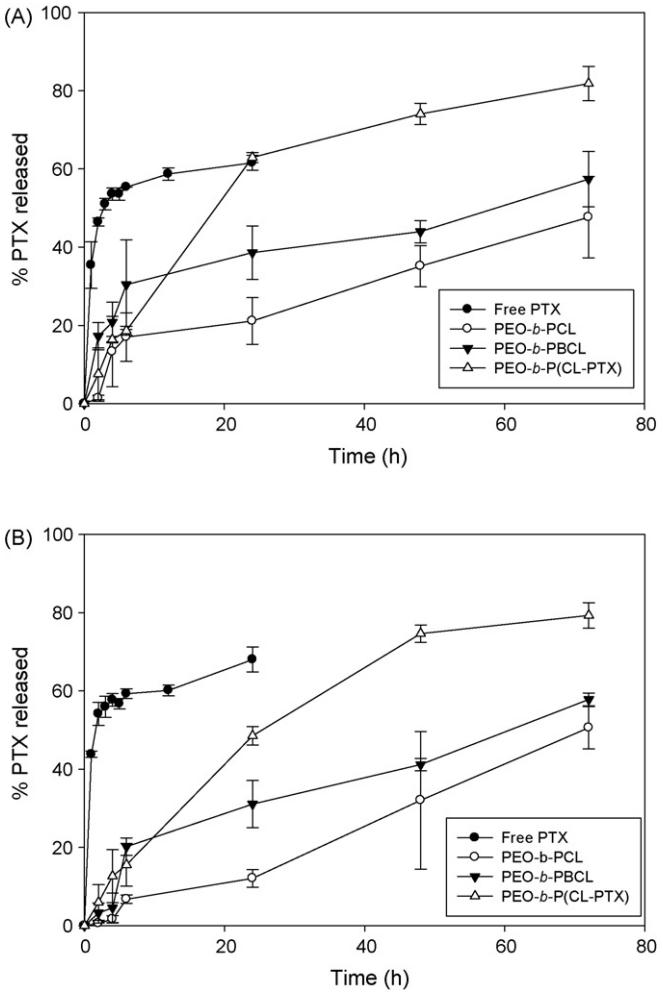

Fig. 7. *In vitro* release profile of physically loaded PTX from different micellar formulations at (A) pH 7.4 and (B) pH 5.0 at 37 °C. Each point represents mean ± SD ($n = 3$).

tively, above which solubility decreased. This ratio coincided with the formation of precipitates. In contrast, PTX solubilization by PEO-*b*-P(CL-PTX) kept increasing as the drug to polymer ratio was raised from 1.34 to 6.67 wt% (the latter was the maximum PTX/polymer wt% examined). Overall, a maximum PTX solubility of 44.5, 32.7, 62.1 μg/mL has been achieved with PEO-*b*-PCL, PEO-*b*-PBCL and PEO-*b*-P(CL-PTX) block copolymers, respectively, at polymer concentrations under study. The calculated loading content of PTX (mole of PTX/mole of polymer) in PEO-*b*-PCL micelles was 14.5. Compared to PEO-*b*-PCL, PTX loading content was increased in PEO-*b*-P(CL-PTX) micelles (by 1.4 folds), but this value decreased in PEO-*b*-PBCL (Table 2). PTX loading did not cause any significant change in the average diameter of PEO-*b*-PCL and PEO-*b*-PBCL ($P > 0.05$, unpaired Student's *t*-test) while PTX loading led to a significant increase in the average diameter of PEO-*b*-P(CL-PTX) particles ($P < 0.01$, unpaired Student's *t*-test) (Table 2). The PTX loaded PEO-*b*-PCL or PEO-*b*-PBCL micelles did not show any secondary aggregation. However, physical encapsulation of PTX into PEO-*b*-P(CL-PTX) resulted in the production of particles which showed signs of secondary aggregation.

The results of assessments on the *in vitro* release of PTX from three different polymeric nano-carriers and free PTX in phosphate (pH 7.4, 0.01 M) and citrate buffer (pH 5.0, 0.01 M) at 37 °C is illustrated in Fig. 7A and B, respectively. Free PTX was released from the dialysis bag at a rapid rate, which means that the transfer of PTX through dialysis membrane to buffer solution is not a

Table 2
Characteristics of PTX loaded copolymer micelles ($n = 3$).

Block copolymer micelles	PTX loading content (%) ± SD		Encapsulation efficiency% ± SD	Average diameter ± SD	PDI[a]	PTX release after 72 h (%)[b]	
	PTX/polymer (mol%)	PTX/polymer (wt%)				pH 5.0	pH 7.4
PEO_{114}-*b*-PCL_{42}	14.5 ± 1.0	1.26 ± 0.09	24.7% ± 3.10	69.2 ± 15.98	0.51	50.6 ± 4.98	47.6 ± 8.68
PEO_{114}-*b*-$PBCL_{18}$	10.7 ± 3.2*	0.96 ± 0.29*	36.4% ± 1.20*	61.0 ± 1.2	0.45	58.8 ± 1.13*	57.4 ± 6.71
PEO_{114}-*b*-P(CL-PTX)$_8$	20.2 ± 2.8[c,*]	2.22 ± 0.31[c,*]	34.0% ± 3.40*	159.3 ± 8.7[d,*]	0.54	79.3 ± 3.23*	81.8 ± 3.81*

[a] Polydispesity index of micellar size distribution.
[b] Release study was performed in citrate buffer (pH 5.0) and in phosphate buffer (pH 7.4).
[c] The level is estimated for physically encapsulated PTX only.
[d] Secondary aggregation was evident.
* Significantly different from PEO-*b*-PCL ($P < 0.05$).

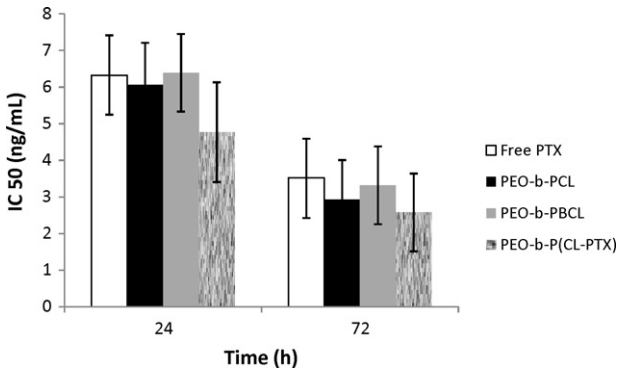

Fig. 8. *In vitro* cytotoxicity of free and physically loaded PTX micellar formulations against MDA-435 after 24 h and 72 h of incubation. Each point represent mean $IC_{50} \pm SE$ ($n = 3$).

restricting factor and the release of PTX from the micellar formulation is the rate limiting step in this process. Comparison of the release profiles of free PTX revealed similar release profiles at pH 7.4 and 5.0 ($f_2 > 50$). The release of PTX from polymeric micelles at both pHs was strongly affected by the micellar core composition, with PEO-*b*-PCL showing the minimum rate of drug release at both pHs. At pH 5.0, changing the core composition significantly affected the percentage of PTX released after 6 h incubation (one-way ANOVA, $P < 0.05$). At 6 h incubation at this pH, 6.80, 20.2 and 15.6% of physically loaded PTX was released from PCL, PBCL and P(CL-PTX) containing particles, respectively. Before 6 h, release rates were similar between different carriers. At pH 7.4; however, differences between release of PTX from nano-carriers was only obvious after 24 h incubation (one-way ANOVA, $P < 0.05$). At pH 7.4 and after 24 h incubation, 21.1, 38.6 and 62.9% of physically loaded PTX were released from PCL, PBCL and P(CL-PTX) containing particles, respectively. At the same time point, 12.1, 31.1 and 48.5% of encapsulated PTX were released from PEO-*b*-PCL, PEO-*b*-PBCL and PEO-*b*-P(CL-PTX) particles at pH 5.0, respectively. Similar to what has been observed for free PTX, comparing the release profiles of physically loaded PTX from polymeric micelles at different pHs using the similarity factor (f_2) showed that the release of PTX from different nano-carriers is not affected by pH ($f_2 > 50$).

The results of *in vitro* cytotoxicity of physically loaded PTX in PEO-*b*-PCL, PEO-*b*-PBCL and PEO-*b*-P(CL-PTX) after 24 and 72 h of incubation are shown in Fig. 8. At all studied incubation times, the physically loaded PTX formulations had similar cytotoxicity against MDA-435 cancer cells to that of free PTX, reflected by similar IC_{50} values ($P < 0.05$, one-way ANOVA test). This observation is attributed to the low equivalent polymer concentrations, which were below the CMC values, under conditions of the cytotoxicity study and rapid release of free PTX from formulations below CMC.

4. Discussion

The long term objective of this research is to develop a biodegradable and biocompatible polymeric carrier in nanometer size range for efficient solubilization and tumor targeted delivery of PTX. An optimized PTX delivery system is expected to act as an efficient and safe solubilizing agent for PTX, be able to prevent early elimination of drug from systemic circulation, reduce PTX exposure and toxicity in non-target sites, but enhance the access of PTX to its cellular and molecular targets. To fulfill these characteristics, two PTX polymeric conjugates, through esterification of PTX with PGA (in Xyotax™) or attachments of PTX to hydroxypropyl methacrylamide polymer through peptide linkers (in PNU166945), have been developed and entered clinical trials. PNU166945 have shown poor pharmacokinetics due to premature drug release as a result of the instability of ester linkage between PTX and polymer in phase I clinical trials. In contrast, Xyotax™ has shown low drug release *in vitro* (<14% after 24 h incubation in buffered saline and plasma) and reduced PTX side effects *in vivo* (Singer et al., 2005). This formulation showed better efficacy compared to that of Taxol® when administered at its maximum tolerable dose which was significantly higher than that of Taxol®, in preclinical and clinical trials.

The PEO-*b*-P(CL-PTX) nano-conjugate developed here is expected to provide several advantages over clinical PTX polymer conjugates. First, the self-association of PEO-*b*-P(CL-PTX) to nanoparticles is expected to stabilize the conjugated PTX within its carrier. Because unlike previous formulations, the ester bond conjugating PTX to polymeric backbone is hidden in the hydrophobic domain of nanoparticles and is not easily accessible for cleavage. Furthermore, the hydrophobicity of PCL structure is anticipated to cause further delay in the dissociation of carrier and/or release of PTX from PEO-*b*-P(CL-PTX) nano-conjugates in comparison to previous clinical PTX polymer conjugates. Owing to the larger size of particles compared to single polymer–PTX chains, the elimination of PEO-*b*-P(CL-PTX) nanoparticles through glomerular filtration will be postponed. Meanwhile, the "stealth" properties induced by the PEO shell is expected to prevent opsonisation and early removal of PEO-*b*-P(CL-PTX) carrier by mononuclear phagocytic system. To achieve similar benefits, direct conjugation of PTX to PEO (at different molecular weights) producing PEO-PTX conjugates has also been pursued previously (Greenwald et al., 1996; Pendri et al., 1998). Overall, compared to clinical conjugates of PTX, a better pharmacokinetic profile for PEO-*b*-P(CL-PTX) leading to improved tumor accumulation is anticipated. On the other hand, unlike poly(methacrylamide) and PGA, which are the building blocks of PNU166945 and Xyotax™, respectively, the PCL backbone is readily degradable in extra-cellular or endosomal environment. Degradability of the polymer backbone in addition to the acid liable linkages between PTX and PCL was hypothesized to provide sufficient release of PTX from the polymeric conjugate in the tumor micro-environment as well as endosomes of tumor cells that have acidic pHs and contain esterase.

In our observations, the PEO-*b*-P(CL-PTX) has illustrated a high tendency for self-assembly reflected by a relatively low CMC (Table 1). Meanwhile, the introduction of PTX substituent on the PCL chain lowered the viscosity of the hydrophobic domains in PEO-*b*-P(CL-PTX) particles (Table 1), possibly due to the increased space between chain entanglements and reduced packing of the hydrophobic chains leading to more freedom of movement in the micellar core. The presence of bulky PTX substituent in the inner core also resulted in the formation of micelles with a larger average diameter (Table 2). Similar effect has been observed in PEO-*b*-poly(α-cholesteryl carboxylate ε-caprolactone) micelles (Mahmud et al., 2009). Despite this, the size of PEO-*b*-P(CL-PTX) particles was still in the appropriate range for tumor targeting by EPR effect (<150 nm) (Table 2). Besides, the particles did not show any sign of aggregation or dissociation during storage at room temperature (Fig. 3). The average micelle size measured by DLS technique was larger than that obtained by TEM or AFM (Fig. 2). This observation has been attributed to the acquirement of the TEM, AFM images under a dry state as opposed to DLS that measures particle size in a hydrated state in aqueous solutions (Hans et al., 2005; Yao et al., 2008). Besides, in TEM and AFM only the dense core of the micelle is visualized without any contribution from the hydrated hydrophilic PEO shell. The difference between AFM and TEM measurements may be attributed to the difference in the interfacial interaction between the nanoparticles and different surfaces and/or different concentration of polymeric nanoparticles used for the two methods (1 mg/mL for TEM vs. 0.1 mg/mL for AFM).

The results of our *in vitro* studies on PTX release revealed the efficient protection of PTX by its PEO-*b*-P(CL-PTX) nano-conjugate preventing the premature release of PTX and its stabilization within the nano-carrier in physiological conditions mimicking that of systemic circulation (pH 7.4 and temperature of 37 °C) (Fig. 4A). Despite degradability of the PCL backbone in acidic pHs mimicking that of tumor tissue or endosomal pH (pH 5.0) (Fig. 4B), release of free PTX from this carrier was found to be too low (Fig. 4A) to provide efficient cytotoxicity in cancer cells even upon prolonged exposure (Fig. 5). The latter was characterized by a high IC_{50} for PEO-*b*-P(CL-PTX) in comparison to free PTX at 72 h incubation (Fig. 5). Although IC_{50} of polymer–PTX conjugate dropped significantly after 96 h incubation, it was still significantly higher than that of free PTX. The low extent of PTX release from the PEO-*b*-P(CL-PTX) nano-conjugate is perhaps due to high hydrophobicity of the micellar core, which retards the diffusion of water into the core and subsequent cleavage of the hydrolysable ester bonds between polymer and PTX. The slow uptake of PEO-*b*-P(CL-PTX) nano-conjugate by cancer cells because of the protective effect of PEO, may contribute to the reduced and time dependent cytotoxicity of PEO-*b*-P(CL-PTX) nano-conjugate, as well. In this regard, further optimization of this carrier, which is currently underway in our research group, will focus on the modification of the surface PEO-*b*-P(CL-PTX) with cancer targeting ligands to improve the cancer cell selective uptake, release and cytotoxic effects of this formulation. Nevertheless, final verdict on the promise of this formulation for successful PTX delivery in cancer can only be made after completion of *in vivo* pharmacokinetics, toxicity and efficacy studies. In fact, Xyotax™ has also shown low PTX release *in vitro* but was found to enhance the therapeutic index of PTX *in vivo*. This is because the *in vitro* condition of the experiment does not provide a precise mimic of the *in vivo* situation where enhanced accumulation of the carriers in tumor site as a result of EPR effect and the presence of additional physiological degradation mechanisms such as metabolizing enzymes, may play a role in modifying the therapeutic index of PTX by its nano-formulation. Such studies are currently under way.

In an effort to find the best structure for the delivery of PTX, PEO-*b*-PCL micelles as well as micelles with modified PCL cores, i.e., PEO-*b*-PBCL and PEO-*b*-P(CL-PTX), were used to physically encapsulate PTX. For PEO-*b*-PCL and PEO-*b*-PBCL block copolymers, the amount of drug solubilized increased up to a maximum concentration, above which drug as well as polymer precipitated (Fig. 6). The solubility profile did not take an exponential curve with a plateau after certain drug: polymer ratio possibly because of polymer/drug precipitation after the point of maximum drug solubility. Micelles containing chemically conjugated PTX demonstrated the highest capacity for physical entrapment of free PTX among structures under study. This observation was similar to observation by Yokoyama et al. (1998) who reported a significant increase in DOX loading by micelles of PEO-*b*-poly(aspartic acid-DOX). The low solubility of PTX in PCL block copolymer has been ascribed to the low compatibility between PTX and PCL, as determined by the calculated Flory Huggin interaction parameter (Letchford et al., 2008). Micelles of PEO-*b*-PBCL even showed lower PTX encapsulation to that obtained by PEO-*b*-PCL micelles, which may be ascribed to the higher rigidity of the core in PEO-*b*-PBCL micelles.

In contrast to chemically conjugated PTX, more rapid loss of physically loaded PTX from its carriers was detected during the release study. The release profile of free and physically encapsulated PTX was not affected by the pH of the release medium. In general, the release of physically encapsulated PTX from its carrier is dependent on both the rate of drug diffusion from micellar core and core degradation; whereas for conjugated PTX, core degradation plays a major role. The nature of core structure significantly affected the rate of PTX release from its carriers. The high rate of PTX release from P(CL-PTX) core in comparison to PCL core may be a reflection of the lower core rigidity for PEO-*b*-P(CL-PTX) micelles.

A comparable cytotoxicity for the physically loaded and free PTX against MDA-MB-435 cells was observed after 24 h incubation. At the reported IC_{50} values for physically encapsulated PTX, the block copolymers' concentrations were below CMC. Therefore, PTX is likely present in its free form. The similar IC_{50} values, only reflects dissociation of all micellar formulations under study within 24–72 h rather than a similarity in PTX release and cell penetration between encapsulated PTX in different micellar structures. Pharmacokinetics studies on these formulations are underway to define the stability of formulations and their potential of targeted PTX delivery in a biological system.

5. Conclusions

In this study, a novel self-associating PTX polymeric conjugate has been successfully prepared with a high loading of PTX. This polymeric conjugate showed sign of PCL chain cleavage only at pH 5.0 (not pH of 7.4). However, cleavage of the ester bond between PTX and PCL leading to the release of intact PTX was very slow and insufficient at both pHs of 7.4 and 5.0. The *in vitro* cytotoxicity of this polymeric conjugate was lower than that of free PTX even after 4 days of incubation with MDA-MB-435 human cancer cells. From the polymeric micellar systems used for the physical encapsulation of PTX, PEO-*b*-P(CL-PTX) micelles significantly improved the solubilization of PTX, while maximum control over the rate of PTX release was achieved with PEO-*b*-PCL micelles. The results point to the potential of self-associating PEO-*b*-PCL based conjugates and containers as nano-carriers for the solubilization and controlled delivery of PTX. *In vivo* studies are needed to determine whether these formulations can in fact improve the therapeutic efficacy of PTX in cancer models.

Acknowledgements

Funding for this research was provided by Natural Science and Engineering Council of Canada (NSERC). The authors would like to acknowledge technical assistance from Dr. A Mahmud and Ms. Sara El-Hasi in polymer synthesis and AFM experiments. Mostafa Shahin acknowledges funding by Frederick Banting and Charles Best CGS Doctoral Award/CIHR and Egyptian Government Scholarship.

References

Boyle, D.A., Goldspiel, B.R., 1998. A review of paclitaxel (Taxol) administration, stability, and compatibility issues. Clin. J. Oncol. Nurs. 2, 141–145.
Chen, Q., Zhang, Q.Z., Liu, J., Li, L.Q., Zhao, W.H., Wang, Y.J., Zhou, Q.H., Li, L., 2003. Multi-center prospective randomized trial on paclitaxel liposome and traditional taxol in the treatment of breast cancer and non-small-cell lung cancer. Chin. J. Oncol. 25, 190–192.
Cho, Y., Lee, J., Lee, S., Huh, K., Park, K., 2004. Hydrotropic agents for study of in vitro paclitaxel release from polymeric micelles. J. Control. Release 97, 249–257.
Costa, P., Sousa Lobo, J.M., 2001. Modeling and comparison of dissolution profiles. Eur. J. Pharm. Sci. 13, 123–133.
Duncan, R., 2003. The dawning era of polymer therapeutics. Nat. Rev. Drug Discov. 2, 347–360.
Duncan, R., 2006. Polymer conjugates as anticancer nanomedicines. Nat. Rev. Cancer 6, 688–701.
Edelman, M.J., 2009. Novel taxane formulations and microtubule-binding agents in non-small-cell lung cancer. Clin. Lung Cancer 10, S30–34.
Forrest, M.L., Yanez, J.A., Remsberg, C.M., Ohgami, Y., Kwon, G.S., Davies, N.M., 2008. Paclitaxel prodrugs with sustained release and high solubility in poly(ethylene glycol)-*b*-poly(epsilon-caprolactone) micelle nanocarriers: pharmacokinetic disposition, tolerability, and cytotoxicity. Pharm. Res. 25, 194–206.
Goldspiel, B.R., 1997. Clinical overview of the taxanes. Pharmacotherapy 17, 110S–125S.
Greenwald, R.B., Pendri, A., Bolikal, D., Gilbert, C.W., 1994. Highly water soluble taxol derivatives: 2′-polyethyleneglycol esters as potential prodrugs. Bioorg. Med. Chem. Lett. 4, 2465–2470.

Greenwald, R.B., Gilbert, C.W., Pendri, A., Conover, C.D., Xia, J., Martinez, A., 1996. Drug delivery systems: water soluble taxol 2′-poly(ethylene glycol) ester prodrugs—design and in vivo effectiveness. J. Med. Chem. 39, 424–431.

Gregory, R.E., DeLisa, A.F., 1993. Paclitaxel: a new antineoplastic agent for refractory ovarian cancer. Clin. Pharm. 12, 401–415.

Hans, M., Shimoni, K., Danino, D., Siegel, S.J., Lowman, A., 2005. Synthesis and characterization of mPEG-PLA prodrug micelles. Biomacromolecules 6, 2708–2717.

Hu, F.-Q., Ren, G.-F., Yuan, H., Du, Y.-Z., Zeng, S., 2006. Shell cross-linked stearic acid grafted chitosan oligosaccharide self-aggregated micelles for controlled release of paclitaxel. Colloids Surf. B: Biointerfaces 50, 97–103.

Langer, C.J., 2004. CT-2103: a novel macromolecular taxane with potential advantages compared with conventional taxanes. Clin. Lung Cancer 6, S85–88.

Lavasanifar, A., Samuel, J., Kwon, G.S., 2001. The effect of alkyl core structure on micellar properties of poly(ethylene oxide)-block-poly(L-aspartamide) derivatives. Colloids Surf. B: Biointerfaces 22, 115–126.

Letchford, K., Liggins, R., Burt, H., 2008. Solubilization of hydrophobic drugs by methoxy poly(ethylene glycol)-block-polycaprolactone diblock copolymer micelles: theoretical and experimental data and correlations. J. Pharm. Sci. 97, 1179–1190.

Letchford, K., Liggins, R., Wasan, K., Burt, H., 2009. In vitro human plasma distribution of nanoparticulate paclitaxel is dependent on the physicochemical properties of poly(ethylene glycol)-block-poly(caprolactone) nanoparticles. Eur. J. Pharm. Biopharm. 71, 196–206.

Li, Y., Kwon, G.S., 1999. Micelle-like structures of poly (ethylene oxide)-block-poly (2-hydroxyethyl aspartamide)-methotrexate conjugates. Colloids Surf. B: Biointerfaces 16, 217–226.

Mahmud, A., Xiong, X.B., Lavasanifar, A., 2006. Novel self-associating poly(ethylene oxide)-block-poly ([epsilon]-caprolactone) block copolymers with functional side groups on the polyester block for drug delivery. Macromolecules 39, 9419–9428.

Mahmud, A., Xiong, X.B., Lavasanifar, A., 2008. Development of novel polymeric micellar drug conjugates and nano-containers with hydrolyzable core structure for doxorubicin delivery. Eur. J. Pharm. Biopharm. 69, 923–934.

Mahmud, A., Patel, S., Molavi, O., Choi, P., Samuel, J., Lavasanifar, A., 2009. Self-associating poly(ethylene oxide)-*b*-poly(alpha-cholesteryl carboxylate-epsilon-caprolactone) block copolymer for the solubilization of STAT-3 inhibitor cucurbitacin I. Biomacromolecules.

Mazzo, D.J., Nguyen-Huu, J.J., Pagniez, S., Denis, P., 1997. Compatibility of docetaxel and paclitaxel in intravenous solutions with polyvinyl chloride infusion materials. Am. J. Health Syst. Pharm. 54, 566–569.

Meerum Terwogt, J.M., ten Bokkel Huinink, W.W., Schellens, J.H., Schot, M., Mandjes, I.A., Zurlo, M.G., Rocchetti, M., Rosing, H., Koopman, F.J., Beijnen, J.H., 2001. Phase I clinical and pharmacokinetic study of PNU166945, a novel water-soluble polymer-conjugated prodrug of paclitaxel. Anticancer Drugs 12, 315–323.

Onetto, N., Canetta, R., Winograd, B., Catane, R., Dougan, M., Grechko, J., Burroughs, J., Rozencweig, M., 1993. Overview of Taxol safety. J. Natl. Cancer Inst. Monogr., 131–139.

Pendri, A., Conover, C.D., Greenwald, R.B., 1998. Antitumor activity of paclitaxel-2′-glycinate conjugated to poly(ethylene glycol): a water-soluble prodrug. Anticancer Drug Des. 13, 387–395.

Ringel, I., Horwitz, S.B., 1987. Taxol is converted to 7-epitaxol, a biologically active isomer, in cell culture medium. J. Pharmacol. Exp. Ther. 242, 692–698.

Sharma, U.S., Balasubramanian, S.V., Straubinger, R.M., 1995. Pharmaceutical and physical properties of paclitaxel (Taxol) complexes with cyclodextrins. J. Pharm. Sci. 84, 1223–1230.

Singer, J.W., 2005. Paclitaxel poliglumex (XYOTAXCT-2103): a macromolecular taxane. J. Control. Release 109, 120–126.

Singer, J.W., Baker, B., De Vries, P., Kumar, A., Shaffer, S., Vawter, E., Bolton, M., Garzone, P., 2003. Poly-(L)-glutamic acid-paclitaxel (CT-2103) [XYOTAX], a biodegradable polymeric drug conjugate: characterization, preclinical pharmacology, and preliminary clinical data. Adv. Exp. Med. Biol. 519, 81–99.

Singer, J.W., Shaffer, S., Baker, B., Bernareggi, A., Stromatt, S., Nienstedt, D., Besman, M., 2005. Paclitaxel poliglumex (XYOTAX; CT-2103): an intracellularly targeted taxane. Anticancer Drugs 16, 243–254.

Singla, A., Garg, A., Aggarwal, D., 2002. Paclitaxel and its formulations. Int. J. Pharm. 235, 179–192.

Skwarczynski, M., Hayashi, Y., Kiso, Y., 2006. Paclitaxel prodrugs: toward smarter delivery of anticancer agents. J. Med. Chem. 49, 7253–7269.

Sparreboom, A., van Zuylen, L., Brouwer, E., Loos, W., de Bruijn, P., Gelderblom, H., Pillay, M., Nooter, K., Stoter, G., Verweij, J., 1999. Cremophor EL-mediated alteration of paclitaxel distribution in human blood: clinical pharmacokinetic implications. Cancer Res. 59, 1454–1457.

Vaisman, B., Shikanov, A., Domb, A.J., 2005. Normal phase high performance liquid chromatography for determination of paclitaxel incorporated in a lipophilic polymer matrix. J. Chromatogr. A 1064, 85–95.

Wall, M.E., Wani, M.C., 1995. Camptothecin and taxol: discovery to clinic—thirteenth Bruce F. Cain Memorial Award Lecture. Cancer Res. 55, 753–760.

Yao, J.H., Mya, K.Y., Li, X., Parameswaran, M., Xu, Q.-H., Loh, K.P., Chen, Z.-K., 2008. Light scattering and luminescence studies on self-aggregation behavior of amphiphilic copolymer micelles. J. Phys. Chem. B 112, 749–755.

Yokoyama, M., Fukushima, S., Uehara, R., Okamoto, K., Kataoka, K., Sakurai, Y., Okano, T., 1998. Characterization of physical entrapment and chemical conjugation of adriamycin in polymeric micelles and their design for in vivo delivery to a solid tumor. J. Control. Release 50, 79–92.

Zhao, C.L., Winnik, M.A., Riess, G., Croucher, M.D., 1990. Fluorescence probe techniques used to study micelle formation in water-soluble block copolymers. Langmuir 6, 514–516.